HIGH EFFICIENCY LASER ION ACCELERATION IN LOW DENSITY PLASMAS

E. d'Humières#, V. Tikhonchuk, Université de Bordeaux-CNRS-CEA, CELIA, Talence, France.

Abstract

Laser driven sources of high energy ions commonly use thin solid foils. A gaseous target can also produce ion beams with characteristics comparable to those obtained with solid targets. Using Particle-In-Cell simulations, we have studied in detail ion acceleration with high intensity laser pulses interacting with low density plasmas. A two-step acceleration process can be triggered: first, ions are accelerated in volume by electric fields generated by hot electrons, second, the ion energy is boosted in a strong electrostatic shock. 2D and 3D simulations show the potential of this regime. It is possible to model separately these two steps. In the first step a hot electron population and a descending density profile are necessary, and the second step develops if a fast proton wave enters in a low density plasma.

INTRODUCTION

A high intensity laser pulse interacting with a thin dense foil can lead to the production of energetic ions [1,2]. These ion beams of short duration and high density are relevant for the fast ignitor scheme in the inertial confinement fusion concept [3], medical applications [4,5,6], and dense plasma diagnostics and probing [7]. A promising way to accelerate ions to high energies with a laser is to use underdense targets. Compared to solid targets where laser absorption is limited to the target surface, the laser pulse inside low density plasmas heats electrons over a large volume leading to higher laser absorption. This acceleration regime is also advantageous for applications as less debris are produced in each shot and it is better adapted to high repetition rate lasers.

After preliminary theoretical [8] and experimental [9] studies on ion laser acceleration using underdense targets, strong longitudinal proton acceleration has been achieved using high intensity lasers [10]. Acceleration of energetic ions observed in [10] has been explained in terms of strong inductive electric fields due to magnetic fields variations on a steep density gradient [11]. Another acceleration process may be operational on a long descending density profile. Here, a collisionless shock can develop on the rear side of the target and strongly increase the maximum proton energy [12].

Collisionless shocks have already been studied on decreasing density gradients for spherical plasmas [13] and for plasmas located at the back of a solid foil irradiated by a laser [14]. In [15], the development of this shock in underdense plasmas was studied and it was shown that protons can be accelerated efficiently in terms of energy. The low and high intensity limits of the shock regime were also investigated using 2D Particle-In-Cell simulations and the efficiency of this regime was demonstrated. In this article, we model the development of these shocks. Using Particle-In-Cell (PIC) simulations, we studied the two steps composing this acceleration process. In Section 2, we give new insights on the underdense ion shock acceleration mechanism using 2D and 3D Particle-In-Cell simulations. Section 3 is dedicated to a detailed analysis of the two steps of this mechanism using 1D Particle-In-Cell simulations. Section 4 is dedicated to conclusions and perspectives.

2D AND 3D SIMULATIONS OF THE ION UNDERDENSE SHOCK REGIME

In this section, we give new insights on the shock regime of laser underdense ion acceleration using 2D and 3D Particle-In-Cell simulations performed with the code PICLS [16]. The wavelength of the incident pulse is λ=1 μm, its pulse duration 23 fs and its irradiance 3.2×10^{19} W/cm^2. The full-width-at-half-maximum (FWHM) of the focal spot is 6 μm. The pulse interacts with the target in normal incidence. Its electric field is in the simulation plane (p-polarization). The spatial and temporal profiles are truncated Gaussians. The plasma is composed of protons and electrons with a 0.08 nc maximum density, a cosine-square density profile with a 100 μm FWHM in the x-direction and uniform in the y-direction. Here, n_c refers to the critical density (1.1×10^{21} cm^{-3} for λ=1 μm).

The acceleration region of the most energetic protons is located near the laser propagation axis. At t=733 fs after the beginning of the simulation (Fig. 1.a) when the acceleration process is starting, the magnetic field in the z-direction is very strong in the acceleration region. The shock has not yet occurred at that time (Fig. 1.e) and the most energetic protons are being accelerated by a strong electric field also present in that region. This field (Fig. 1.c) is composed both of an inductive field and an electrostatic field due to the hot electron current generated by the laser propagation. At t=1833 fs after the beginning of the simulation (Fig. 1.b), the amplitude of the magnetic field in the z direction has strongly decreased on the laser propagation axis whereas the amplitude of accelerating electric field is still high (Fig. 1.d). In the shock regime, the inductive field can therefore be important at the beginning of the acceleration process but not during the second acceleration step when the shock develops and acts as an additional acceleration process. The density diagnostics show a strong correlation with the high electric field in this second step and a typical shock structure [17] is observed in the proton phase space (Fig. 1.f).

* #dhumieres@celia.u-bordeaux1.fr

Copyright © 2011 by PAC'11 OC/IEEE — cc Creative Commons Attribution 3.0 (CC BY 3.0)

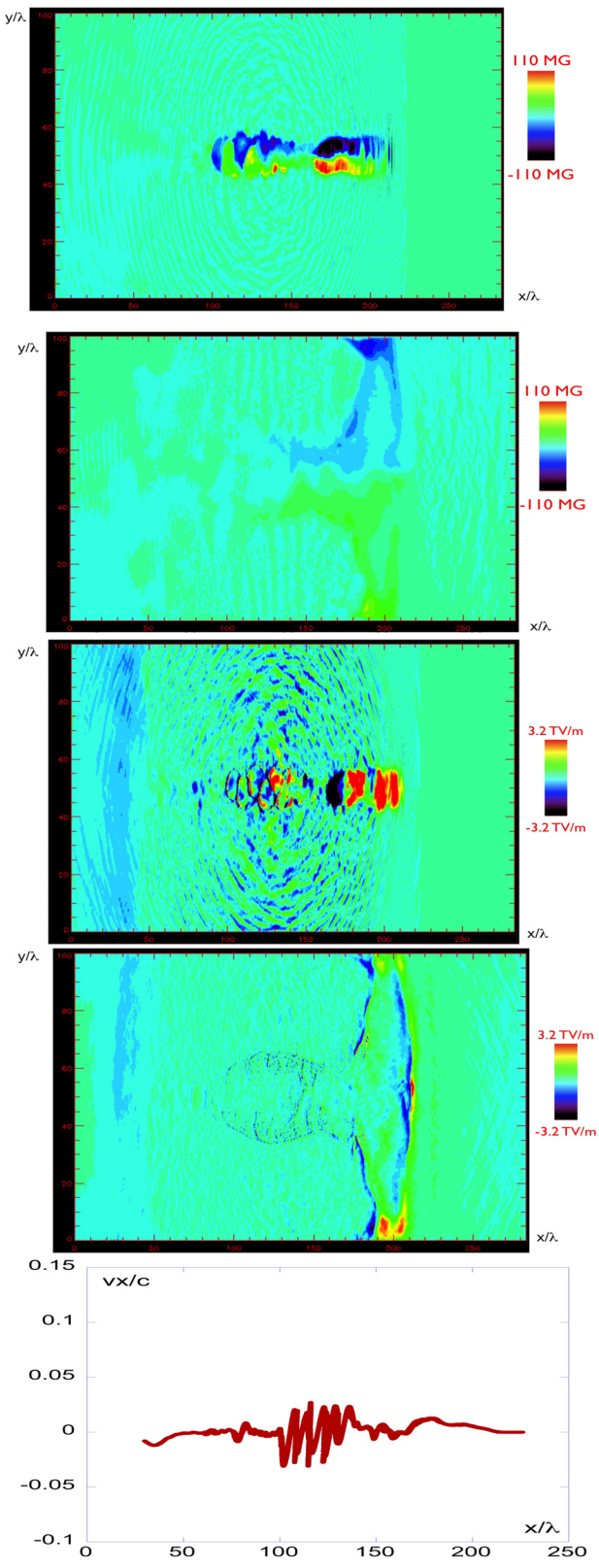

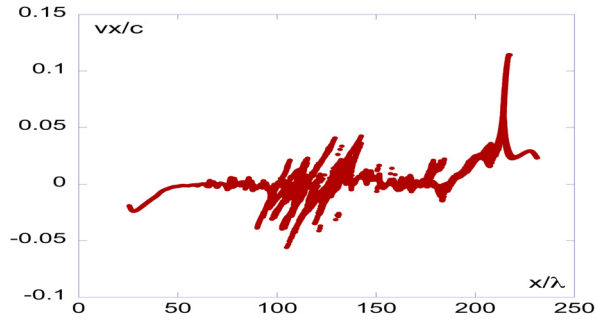

Figure 1: (a,b) 2D map of the B_z magnetic field at t=733 fs and at t=1833 fs. (c,d) 2D map of the E_x electric field at t=733 fs and at t=1833 fs (e,f) Proton phase space at t=733 fs and at t=1833 fs.

We have also performed the first 3D Particle-In-Cell simulation of this regime using the code PICLS [16]. Laser pulse duration is 16 fs and its irradiance 3.2×10^{19} W/cm^2. The plasma is composed of protons and electrons with a 0.08 n_c maximum density, a cosine-square density profile with a 50 μm FWHM in the x-direction and uniform in the y and z directions. All other parameters are the same as in the previous 2D simulation.

The two-step mechanism observed in the previous 2D simulation is also responsible for the acceleration of energetic protons. Maximum proton energy reaches 9 MeV with these parameters (Fig. 2). The acceleration of high energy protons is therefore as efficient as in 2D setups and can therefore be highlighted in experiments. The laser parameters used here are already achievable in several laboratories in the world. The main problem is to produce short low density decreasing density gradients.

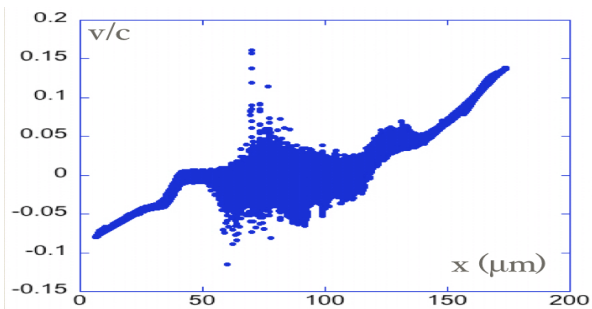

Figure 2: Proton phase space 2.36 ps after the beginning of the 3D simulation.

DETAILED ANALYSIS OF THE TWO STEPS OF THE SHOCK REGIME

The role of the decreasing density gradient and the importance of a background plasma to launch the shock have been respectively highlighted in [12] and [15]. The results of the previous section give a better understanding of the whole two-step process. Using 1D Particle-In-Cell simulations performed with PICLS, two setups were chosen to study separately these two steps. The first step of the acceleration process requires a hot electron population and a descending density profile, and the

Copyright © 2011 by PAC'11 OC/IEEE — cc Creative Commons Attribution 3.0 (CC BY 3.0)

second step develops if the ion bunch resulting from the first step enters in a low density plasma.

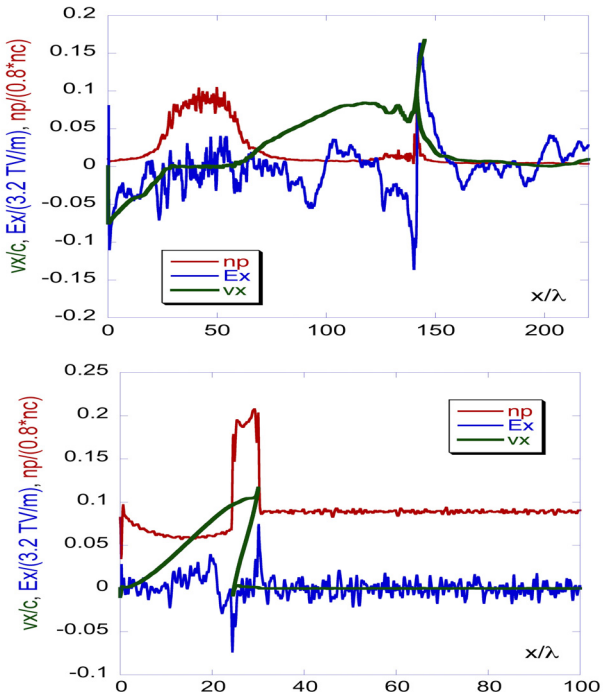

Figure 3: (a) Proton phase space, proton density and longitudinal electric field at t=1.76 ps for an initial hot electron temperature in a decreasing density gradient. (b) Proton phase space, proton density and longitudinal electric field at t=220 fs for a fast proton wave propagating in a constant density profile.

In the first setup, no laser is used. The plasma is composed of protons and electrons with a maximum density of 0.08 nc, and a cosine-square density profile a 40 μm full width at half maximum (FWHM). The right part of the simulation box is filled with a 0.004 nc constant density plasma. The electrons in the decreasing density region have an initial temperature of 4 MeV. The hot electrons quickly start to accelerate protons in the decreasing density gradient. A high velocity ion wave is therefore launched. When this wave propagates through the constant density plasma, proton density increases at the front of the wave and after 1.5 ps a strong electrostatic field appears (Fig. 3.a). A sharp increase in proton velocity quickly follows and a strong electrostatic shock develops. This simulation shows the accuracy of the two step-model discussed above.

In the second setup also, no laser is used. The plasma is composed of protons and electrons with a constant density profile at 0.08 nc. The electron initial temperature is 50 keV. A proton wave with a velocity of 0.1 times the velocity of light is launched from the left boundary. As it propagates in the constant density plasma, the same behaviour observed for the first setup occurs. Proton density increases strongly until a strong electrostatic field develops at the front of the proton wave and an electrostatic shock is launched at t=220 fs (Fig. 3.b). This second setup shows that the second step of the shock regime of laser proton acceleration in underdense plasmas does not require a decreasing density gradient.

CONCLUSIONS

Particle-In-Cell simulations were used to study proton acceleration in underdense targets. The two-step mechanism already described in previous publications has been investigated in more details in the present article. The first step, the launch of a fast ion wave in the decreasing gradient due to a strong longitudinal electric field, has been shown to occur in a zone of high amplitude magnetic fields. In the second step, the development of a strong electrostatic shock, the longitudinal electric field leads to the production of energetic protons. The first 3D simulation of this regime is presented and confirms the 2D simulation results. We have also shown that these two steps can be modelled separately. The first step of the acceleration process requires a hot electron population and a descending density profile, and the second step develops if the ion bunch resulting from the first step enters in a low density plasma. These results could be used to model these processes using a Vlasov-Poisson code and to obtain scaling laws of the maximum proton energy and accelerated proton numbers with laser and target parameters. Even if this regime is nowadays difficult to achieve experimentally, these new results could help find new combinations of parameters to highlight this process. This mechanism could open important perspectives for the optimization of high-energy proton beams and to study low velocity astrophysical shocks.

REFERENCES

[1] E. Clark et al., Phys. Rev. Lett. 84, 670 (2000).
[2] R. A. Snavely et al., Phys. Rev. Lett. 85, 2945 (2000).
[3] M. Roth et al., Phys Rev ST-AB 5, 061002 (2002).
[4] S. Fritzler et al., Appl. Phys. Lett. 83, 3039 (2003).
[5] V. Malka et al., Med. Phys. 31, 6 (2004).
[6] K. W. D. Ledingham et al., J. Phys. D: Appl. Phys. 37, 2341 (2004).
[7] M. Borghesi et al., Phys. Plasmas 9, 2214 (2002).
[8] T. ZH. Esirkepov et al., JETP Lett. 70, 82 (1999), M. Yamagiwa et al., Phys. Rev. E 60, 5987 (1999), Y. Sentoku et al., Phys. Rev. E 62, 7271 (2000).
[9] K. Krushelnick et al., Phys. Rev. Lett. 83,737 (1999), G. S. Sarkisov et al., Phys. Rev. E 59, 7042 (1999).
[10] L. Willingale et al., Phys. Rev. Lett. 96, 245002 (2006), A. Yogo et al., Phys. Rev. E 77, 016401 (2008), P. Antici et al., New J. Phys. 11, 023038 (2009).
[11] S. V. Bulanov et al., Phys. Rev. Lett. 98, 049503 (2007).
[12] E. d'Humières et al., J. Phys.: Conf. Ser. 244, 042023 (2010).
[13] F. Peano et al., Phys. Plasmas 14, 056704 (2007).
[14] V.T. Tikhonchuk et al., Plasma Phys. and Control. Fusion 47, 869 (2005).
[15] E. d'Humières et al., AIP Conf. Proc. 1299, 704 (2010).
[16] Y. Sentoku et al., J. Comput. Phys. 227, 6846 (2008).
[17] D. W. Forslund et al., Phys. Rev. Lett. 25, 1699 (1970), D. W. Forslund et al., Phys. Rev. Lett. 27, 1189 (1971), L. Silva et al., Phys. Rev. Lett. 92, 015002 (2004).

Copyright © 2011 by PAC'11 OC/IEEE — cc Creative Commons Attribution 3.0 (CC BY 3.0)